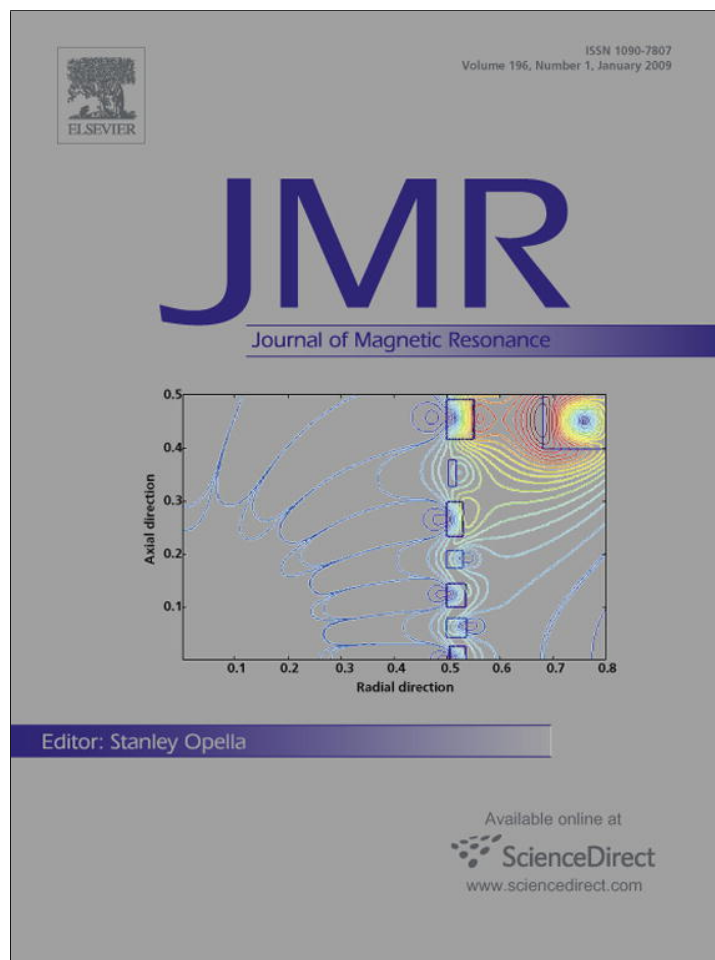


Provided for non-commercial research and education use.  
Not for reproduction, distribution or commercial use.



This article appeared in a journal published by Elsevier. The attached copy is furnished to the author for internal non-commercial research and education use, including for instruction at the authors institution and sharing with colleagues.

Other uses, including reproduction and distribution, or selling or licensing copies, or posting to personal, institutional or third party websites are prohibited.

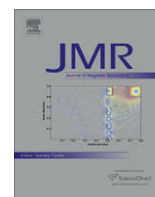
In most cases authors are permitted to post their version of the article (e.g. in Word or Tex form) to their personal website or institutional repository. Authors requiring further information regarding Elsevier's archiving and manuscript policies are encouraged to visit:

<http://www.elsevier.com/copyright>



Contents lists available at ScienceDirect

## Journal of Magnetic Resonance

journal homepage: [www.elsevier.com/locate/jmr](http://www.elsevier.com/locate/jmr)

## 2D $^1\text{H}$ – $^{31}\text{P}$ solid-state NMR studies of the dependence of inter-bilayer water dynamics on lipid headgroup structure and membrane peptides

Tim Doherty, Mei Hong\*

Department of Chemistry, Iowa State University, Gilman 108, Ames, IA 50011, USA

## ARTICLE INFO

## Article history:

Received 5 August 2008

Revised 29 September 2008

Available online 5 October 2008

## Keywords:

Water

Lipid membranes

Solid-state NMR

 $^1\text{H}$ – $^{31}\text{P}$  correlation

Membrane proteins

Dynamics

## ABSTRACT

The dynamics of hydration-water in several phospholipid membranes of different compositions is studied by 2D  $^1\text{H}$ – $^{31}\text{P}$  heteronuclear correlation NMR under magic-angle spinning. By using a  $^1\text{H}$   $T_2$  filter before and a  $^1\text{H}$  mixing-time after the evolution period and  $^{31}\text{P}$  detection, inter-bilayer water is selectively detected without resonance overlap from bulk water outside the multilamellar vesicles. Moreover the  $^1\text{H}$   $T_2$  relaxation time of the inter-bilayer water is measured. Lipid membranes with labile protons either in the lipid headgroup or in sterols exhibit water– $^{31}\text{P}$  correlation peaks while membranes free of exchangeable protons do not, indicating that the mechanism for water–lipid correlation is chemical exchange followed by relayed magnetization transfer to  $^{31}\text{P}$ . In the absence of membrane proteins, the inter-bilayer water  $^1\text{H}$   $T_2$ 's are several tens of milliseconds. Incorporation of charged membrane peptides shortened this inter-bilayer water  $T_2$  significantly. This  $T_2$  reduction is attributed to the peptides' exchangeable protons, molecular motion and intermolecular hydrogen bonding, which affect the water dynamics and the chemically relayed magnetization transfer process.

© 2008 Elsevier Inc. All rights reserved.

### 1. Introduction

Water is essential to the structure and dynamics of biological molecules. The folding, dynamics and function of proteins and nucleic acids are strongly influenced by water. The self-assembly of amphipathic lipid molecules to form the bilayer that protects all cells also requires water. The hydration force between lipid bilayers has long been recognized as an important factor that influences the physical properties of lipid membranes [1,2]. A wide range of biophysical techniques, including  $^2\text{H}$  NMR [3–6],  $^1\text{H}$  NMR [6–9], neutron scattering [10,11], X-ray scattering [12,13], Raman scattering [14], osmotic stress and surface force measurements [2], and molecular dynamics simulations, have been used to characterize the interaction of water with lipid membranes. The most extensively characterized lipid membranes are the phosphatidylcholines (PC), for which both the water dynamics [3,4] and lipid dynamics [15] have been investigated as a function of hydration level and the membrane phase. However, so far few spectroscopic studies have directly compared the dynamics of water in lipids of different headgroups, and the effect of membrane proteins on water–membrane interactions has been scarcely investigated.

High-resolution magic-angle spinning (MAS) NMR spectroscopy is an excellent approach for probing the structure and dynamics of

lipid membranes [16,17]. Due to the fast uniaxial rotational diffusion of lipid molecules, hydrated lipid membranes exhibit well resolved  $^1\text{H}$  spectra under moderate magic-angle spinning, making  $^1\text{H}$  1D and 2D MAS NMR the method of choice for investigating membrane dynamics and disorder [18]. The heteronuclear  $^1\text{H}$ – $^{31}\text{P}$  2D correlation technique is particularly sensitive to membrane-associated water. Since water residence time on the membrane surface is only on the order of 100 ps based on  $^1\text{H}$  NOESY experiment [7], direct dipolar coupling of water with the lipid phosphate group is not sufficiently strong to be detectable by NMR. Instead, water– $^{31}\text{P}$  correlation peaks in 2D spectra reflect water magnetization transferred to some lipid headgroup protons, then relayed to lipid protons closest to  $^{31}\text{P}$  before cross-polarization (CP) to  $^{31}\text{P}$ .

In this work, we probe the water–lipid interaction using the  $^1\text{H}$ – $^{31}\text{P}$  2D correlation experiment and examine the dynamics of the lipid-correlated water by measuring its  $T_2$  relaxation times. A number of membranes with different headgroup structures are studied. They include phosphatidylcholine, phosphatidylethanolamine (PE), and phosphatidylglycerol (PG). Cholesterol is added to one of the PC samples to study the effect of this important sterol on hydration-water dynamics. Mixed PE/PG membranes containing two cationic antimicrobial peptides are then studied to examine the influence of membrane proteins containing polar charged residues on hydration-water dynamics. These membrane composition variations allow us to understand the effects of labile lipid protons, hydrogen bonding, membrane surface charge, sterol, and proteins on the hydration-water dynamics.

\* Corresponding author. Fax: +1 515 294 0105.

E-mail address: [mhong@iastate.edu](mailto:mhong@iastate.edu) (M. Hong).

## 2. Materials and Methods

### 2.1. Membrane sample preparation

All lipids were purchased from Avanti Polar Lipids (Alabaster, AL) and used without further purification. Most samples were prepared by dissolving and mixing the lipids in chloroform, evaporating chloroform under a stream of dry nitrogen gas, then resuspending the lipid mixture in cyclohexane and lyophilizing overnight. Chloroform is necessary for complete mixing of the lipids, while cyclohexane is necessary for complete removal of the organic solvent after mixing. The dried lipid powder was packed into 4-mm MAS rotors and directly hydrated. The amount of water added was approximate 35 wt.% of the total mass. The exact hydration level was determined by integration of the  $^1\text{H}$  NMR spectra. Antimicrobial peptides TP-I and PG-1 were synthesized using standard Fmoc chemistry as described before [19,20], and were reconstituted into POPE/POPG membranes by mixing lipid vesicle solutions with the appropriate amount of the peptide solution. The mixed solution was centrifuged at 150,000g to obtain wet pellets, which were then lyophilized, packed into the rotor, and rehydrated to ~35 wt.% water.

### 2.2. Solid-state NMR experiments

Magic-angle spinning (MAS) NMR experiments were carried out on a Bruker DSX-400 spectrometer (Karlsruhe, Germany) operating at Larmor frequencies of 400.49 MHz for  $^1\text{H}$  and 162.12 MHz for  $^{31}\text{P}$ . An MAS probe equipped with a 4 mm spinner was used for all experiments. The samples were spun at 4.0 kHz in most experiments. Typical  $^1\text{H}$ - $^{31}\text{P}$  cross-polarization (CP) contact times were 4 ms and the Hartmann-Hahn match was established at 50 kHz. The  $^1\text{H}$   $90^\circ$  pulse length was 5  $\mu\text{s}$ , and the  $^1\text{H}$  decoupling field was 42–50 kHz during  $^{31}\text{P}$  detection. Recycle delays for the  $^1\text{H}$ - $^{31}\text{P}$  2D correlation experiments were 2.5–3.0 s. The  $^1\text{H}$  chemical shifts were internally referenced to the lipid chain  $\text{CH}_3$  signal at 0.9 ppm [21].

$^1\text{H}$ -detected water  $T_2$ 's were measured using a 1D Hahn-echo experiment.  $^{31}\text{P}$ -detected water  $T_2$ 's were measured using the 2D  $^1\text{H}$ - $^{31}\text{P}$  correlation experiment with a  $^1\text{H}$  mixing period and a pre-evolution  $T_2$  filter (Fig. 1) [22]. In this experiment,  $^{31}\text{P}$  magnetization is first destroyed by several  $90^\circ$  pulses. A  $^1\text{H}$   $90^\circ$  excitation pulse is then applied, followed by a Hahn-echo period with a variable delay  $2\tau$ .  $^1\text{H}$  chemical shift evolution ( $t_1$ ) ensues, then the  $^1\text{H}$  magnetization is stored along the z-axis for a period  $t_m$ , during which magnetization transfer occurs by either spin diffusion or nuclear Overhauser effect (NOE). Finally, the  $^1\text{H}$  magnetization is cross-polarized to  $^{31}\text{P}$  for detection in  $t_2$ . A series of 2D experiments with varying echo delays  $2\tau$  was conducted to measure the  $T_2$  of the water protons that correlate with the lipid  $^{31}\text{P}$ . Mixing times of 1–225 ms were used in the 2D experiments.

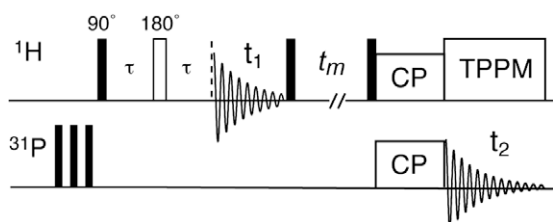


**Fig. 1.** Pulse sequence for the 2D  $^1\text{H}$ - $^{31}\text{P}$  correlation experiment with a  $^1\text{H}$   $T_2$  filter period of  $2\tau$  and a mixing period of  $t_m$ . Filled and open rectangles denote  $90^\circ$  and  $180^\circ$  pulses, respectively.

## 3. Results

### 3.1. 1D $^1\text{H}$ MAS spectra—bulk water and inter-bilayer water

The goal of this study is to investigate the interaction between water and lipid membranes with different headgroups and measure the dynamics of the hydration-water of the membrane. Phospholipids containing palmitoyl and oleoyl chains were used in all samples because these acyl chains are the most abundant in biological membranes. The PC, PE and PG headgroup chemical structures and their nomenclatures are shown in Fig. 2. The three lipids have different gel to liquid-crystalline phase transition temperatures ( $T_m$ ):  $-2^\circ\text{C}$  for POPC and POPG and  $25^\circ\text{C}$  for POPE. The dynamics of hydration-water should depend both on the bulk water property and the membrane dynamics. We chose to conduct the NMR experiments at similar temperatures with respect to their phase transition temperatures ( $T_m$ ). This reduced temperature,  $\Delta T = T - T_m$ , was set to be 5–7  $^\circ\text{C}$  for the various membranes studied (Table 1). For mixed POPE/POPG membranes the weighted molar average of lipids is used to find the  $T_m$  of the mixture.

Fig. 3 shows the 1D  $^1\text{H}$  MAS spectra of the POPC, POPE, and POPE/POPG mixed membranes. The  $^1\text{H}$  peaks are assigned based on literature chemical shift values [23–25] and additional  $^1\text{H}$ - $^{13}\text{C}$  2D correlation spectra measured directly on these samples (not shown). Close inspection of the water region of the  $^1\text{H}$  spectra show two partially resolved peaks—a narrow downfield component and a broad upfield component—for POPC/cholesterol, POPE, and POPG membranes but not for the POPC membrane (Fig. 4). The chemical shift difference between the two components is about 0.05 ppm (Table 2). We assign the sharp peak to mobile bulk water outside the multilamellar vesicles and the broad peak to inter-bilayer water that interacts intimately with the lipids. The partial spectral resolution means that the two types of water are in slow-exchange with rates less than  $0.05 \times 400 \times 2\pi = 125 \text{ s}^{-1}$ , consistent with prior experiments on membranes packed in spherical inserts [8]. Hahn-echo detection with a long echo period preferentially suppressed the broad upfield peak, supporting the presence of two types of water. The  $^1\text{H}$   $T_2$  relaxation times of the two water peaks are listed in Table 1: the broad water  $T_2$  (~20 ms) is an order-of-magnitude shorter than the narrow water  $T_2$  (~400 ms) for the POPC/cholesterol and POPE membranes. For the peptide-containing POPE/POPG membranes, the  $^1\text{H}$   $T_2$ 's of the broad water peak is generally shorter than the pure membranes. The TP-I sample retains the order-of-magnitude difference between the bulk

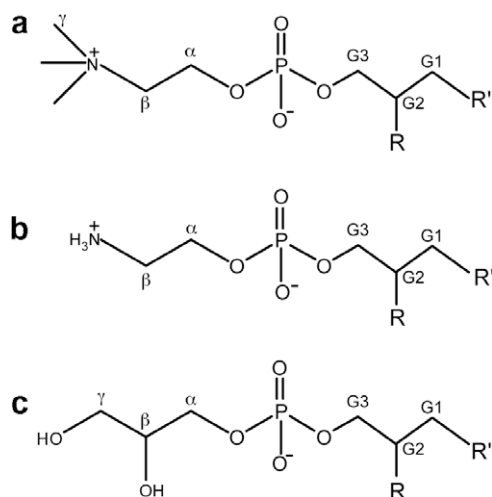


**Fig. 2.** Headgroup structures of the phospholipids used in this study. (a) POPC. (b) POPE. (c) POPG. R and R' denote oleoyl and palmitoyl chains, respectively.

**Table 1**  
Water  $^1\text{H}$   $T_2$  (ms) values observed from 1D  $^1\text{H}$  and 2D  $^1\text{H}$ - $^{31}\text{P}$  spectra, with experimental temperatures.

Membrane	1D, Narrow	1D, Broad	2D	T (°C)	$\Delta T$ (°C)
POPC	—	59 ± 1	—	5	7
POPC/cholesterol (3:2)	375 ± 40	23 ± 1	15 ± 1	5	7
POPE	410 ± 70	18 ± 1	16 ± 2	30	5
POPG	—	32 ± 1	30 ± 3	5	7
POPE/POPG (3:2), POPE	81 ± 4	—	30 ± 2	20	6
POPG	—	—	40 ± 1	20	6
POPE/POPG/TP-1 (9:6:1)	82 ± 1	4.5 ± 0.5	3.3 ± 0.3	20	6
POPE/POPG/PG-1 (8:4:1)	—	16 ± 1	0.4 ± 0.2, 12 ± 1	25	7

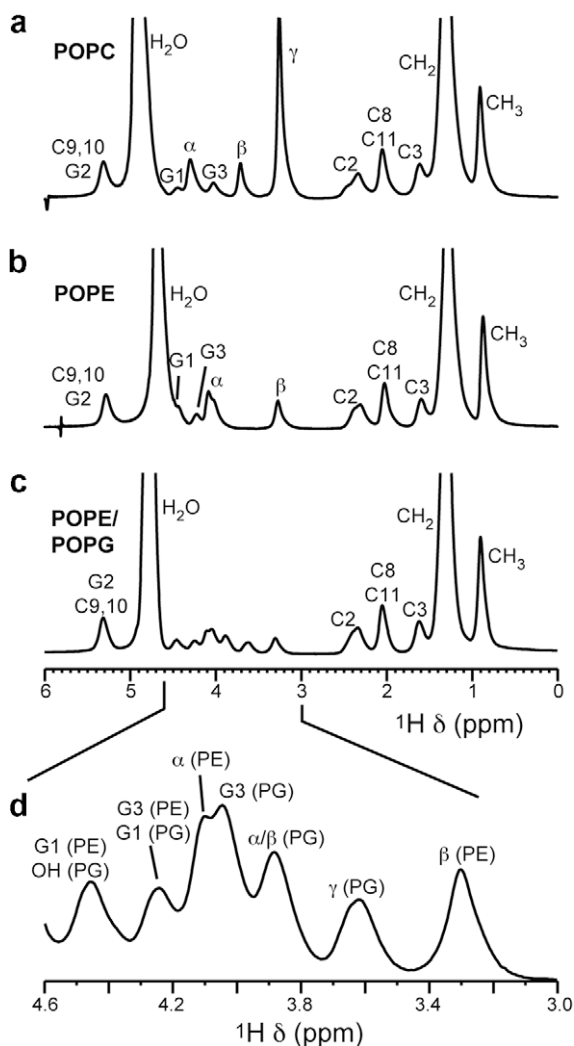


**Fig. 3.** 1D  $^1\text{H}$  MAS spectra of three hydrated lipid membranes. (a) POPC. (b) POPE. (c) POPE/POPG membrane. (d) Inset for the POPE/POPG membrane showing the assignment for the 3.0–4.6 ppm region.

water and inter-bilayer water  $T_2$ . The PG-1 sample shows only a single water peak, with a short  $^1\text{H}$   $T_2$  of 16 ms.

### 3.2. $^1\text{H}$ - $^{31}\text{P}$ 2D correlation spectra— $^1\text{H}$ $T_2$ of the inter-bilayer water

Since 1D  $^1\text{H}$  spectra do not completely resolve the inter-bilayer water signal from the bulk water signal, it is of interest to selectively detect the inter-bilayer water in the absence of the dominant bulk water peak. The 2D  $^1\text{H}$ - $^{31}\text{P}$  correlation experiment with  $^1\text{H}$  mixing [22,26] achieves this purpose and at the same time verifies the assignment of the broad water peak to inter-bilayer water. In

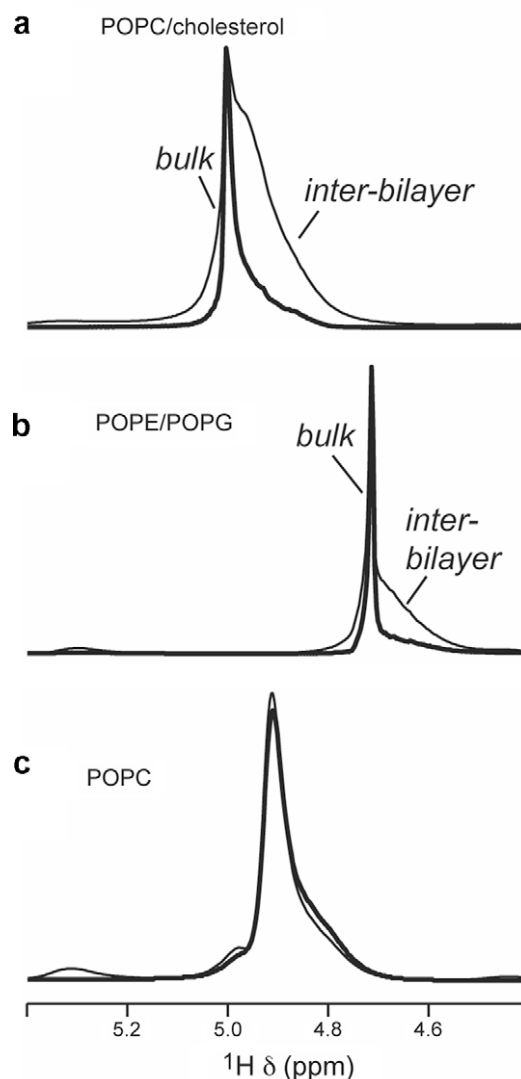


**Fig. 4.** Water region of the 1D direct-excitation  $^1\text{H}$  MAS spectra of lipid membranes without (thin line) and with a  $T_2$  filter (thick line). (a) POPC/cholesterol membrane. The echo delay ( $2\tau$ ) is 80 ms. (b) POPE/POPG (3:2) membrane.  $2\tau = 30$  ms. (c) POPC membrane.  $2\tau = 80$  ms. Note the one-component nature of the POPC spectrum.

this experiment, the  $^1\text{H}$  spins closest to the lipid phosphate group,  $\text{H}\alpha$  and G3, cross-polarize to  $^{31}\text{P}$ . Protons further from the phosphate group, including water, first transfer their magnetization to  $\text{H}\alpha$  and G3 by a number of possible mechanisms, including chemical exchange, spin diffusion, and dipolar cross relaxation (i.e. NOE), then cross-polarize to  $^{31}\text{P}$ . A mixing-time of 64 ms and a  $^1\text{H}$ - $^{31}\text{P}$  CP contact time of 4 ms were typically used in the 2D experiments. When water cross peaks are not detected under these conditions, the mixing-time was extended to 225 ms.

**Table 2**

Water  $^1\text{H}$  chemical shifts (ppm) in various lipid membranes. The bulk water frequencies are obtained from 1D  $^1\text{H}$  spectra, and the inter-bilayer water frequencies are obtained from 2D  $^1\text{H}$ - $^{31}\text{P}$  spectra.

Membrane	Bulk	Inter-bilayer
POPC	—	4.92
POPC/cholesterol (3:2)	5.00	4.94
POPE	4.71	4.66
POPE/POPG (3:2)	4.79	4.71
POPE/POPG/TP-1 (9:6:1)	4.91	4.86
POPE/POPG/PG-1 (8:4:1)	4.80	4.76

Fig. 5 shows two representative  $^1\text{H}$ - $^{31}\text{P}$  2D spectra, for the POPC membrane and the POPE/POPG membrane, and Fig. 6 compares the  $^1\text{H}$  cross sections for six lipid membranes with their respective 1D  $^1\text{H}$  direct-excitation spectra. Several common features are observed in the 2D spectra. First, the strongest  $^1\text{H}$ - $^{31}\text{P}$  cross peaks come from the headgroup  $\text{H}\alpha$  and glycerol G3, as expected due to the proximity of these methylene groups to  $^{31}\text{P}$ . The G3 cross peak is broader and lower than  $\text{H}\alpha$  which is expected because no  $^1\text{H}$  homonuclear decoupling is applied during the evolution time and  $^1\text{H}$ - $^1\text{H}$  dipolar coupling for G3 are a factor of 3.5 times stronger than  $\text{H}\alpha$  due to the nearly parallel orientation of the G3 geminal H-H vector to the lipid motional axis [27]. On the other hand, G3 protons do not cross-polarize much more efficiently than  $\text{H}\alpha$  to  $^{31}\text{P}$  since the  $^1\text{H}$ - $^{31}\text{P}$  dipolar coupling for G3 is only a factor of 1.5 stronger than for  $\text{H}\alpha$  [27]. The second common feature among the spectra is that the acyl chain  $\text{CH}_2$  also exhibits a cross peak with  $^{31}\text{P}$ , indicating chain-headgroup contacts. A significant contribution to this cross peak is intermolecular  $^1\text{H}$ - $^1\text{H}$  NOE due to chain upturns in the fluid bilayer, as shown before for non-cholesterol-containing membranes [28,29]. Finally, water- $^{31}\text{P}$  cross peaks are observed between 4.7 and 5.1 ppm for all membranes except for POPC, and in most cases have lower intensities than the  $\text{H}\alpha$  peaks. This is consistent with the intermolecular nature of the water- $^{31}\text{P}$  magnetization transfer and the high mobility of water.

In the following we describe the water- $^{31}\text{P}$  cross peak for each lipid membrane. The POPC membrane does not exhibit any water- $^{31}\text{P}$  cross peak up to 225 ms mixing (Fig. 6a). We attribute this absence to the lack of exchangeable protons in the POPC head-

group, since all other membranes studied here contain labile protons and exhibit water- $^{31}\text{P}$  cross peaks in the 2D spectra. Negative water-headgroup  $^1\text{H}$ - $^1\text{H}$  cross peaks in 2D NOESY spectra, corresponding to positive water-headgroup cross relaxation rates, have been reported for POPC membranes [7,9]. Thus, the lack of a water- $^{31}\text{P}$  cross peak suggests that the water-headgroup dipolar coupling, while present, is not strong enough to be detected by the current 2D  $^1\text{H}$ - $^{31}\text{P}$  correlation experiment. In addition, the 1D  $^1\text{H}$  spectrum of POPC shows only a single water peak, thus the water signal must come from the inter-bilayer hydration-water rather than the bulk water outside the multilamellar vesicle.

In contrast to the pure POPC membrane, the addition of cholesterol to the POPC membrane gave rise to a strong water cross peak (Fig. 6b) that matches the position of the broad water peak in the 1D spectrum (Fig. 4a). Varying the  $T_2$  filter time of the 2D experiment yielded a  $^{31}\text{P}$ -detected water  $T_2$  of 15 ms, in qualitative agreement with the 1D-detected  $T_2$  (Table 1). We attribute the water cross peak in the POPC/cholesterol membrane to the combined effect of exchange between water and the cholesterol hydroxyl proton and the condensing effect of cholesterol on lipid membranes, which facilitates  $^1\text{H}$  spin diffusion.

The POPE membrane exhibits a weak water cross peak at 4.66 ppm (Fig. 6c) in the 2D spectrum with a 16 ms  $T_2$ , consistent with the 18 ms  $T_2$  found in the 1D spectra. Fig. 7 shows several water  $^1\text{H}$   $T_2$  decay curves detected using the 1D  $^1\text{H}$  and 2D  $^{31}\text{P}$ -detected experiments. The POPE data highlights the spectral simplification by 2D correlation: the 1D  $T_2$  decay is bi-exponential due to the partial overlap of the inter-bilayer and bulk water signals, while the 2D-detected  $T_2$  decay is single exponential, reflecting only the inter-bilayer water dynamics.

For the POPE membrane, the water cross peak most likely results from chemical exchange between water and the headgroup amine protons ( $\text{H}\gamma$ ) followed by relayed magnetization transfer to  $^{31}\text{P}$ . The native  $\text{H}\gamma$ - $^{31}\text{P}$  cross peak, if protected from exchange, would be negligible, since the  $\text{H}\beta$ - $^{31}\text{P}$  cross peak is already very weak. The monotonic intensity decrease of  $^1\text{H}$ - $^{31}\text{P}$  cross peaks from  $\text{H}\alpha$  to  $\text{H}\beta$  and  $\text{H}\gamma$  is clearly seen in the 2D POPC spectrum (Fig. 6a), which does not have resonance overlap between water and  $\text{H}\gamma$ .

To examine the influence of sample preparation methods on hydration-water dynamics, we prepared another POPE sample by

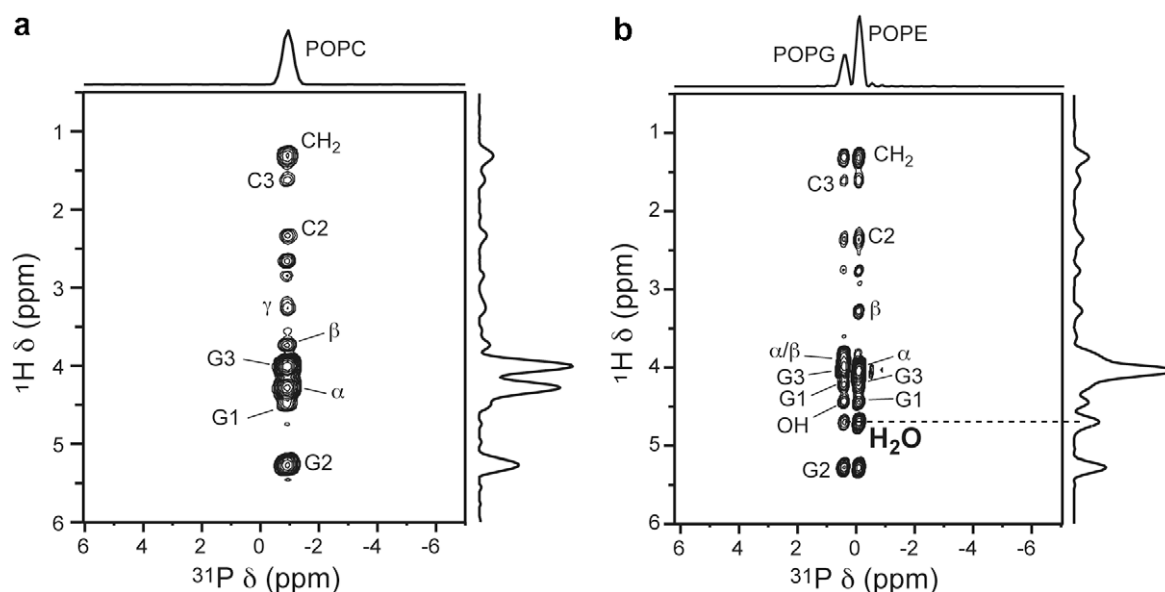


**Fig. 5.** Representative 2D  $^1\text{H}$ - $^{31}\text{P}$  correlation spectra of hydrated lipid membranes with a mixing-time of 64 ms. (a) POPC. (b) POPE/POPG (3:2) membrane.  $^1\text{H}$  peak assignment is indicated. POPC lacks a water- $^{31}\text{P}$  cross peak. Extending the mixing-time to 225 ms still yields no water cross peak. Spectra were measured under 4.0 kHz MAS.

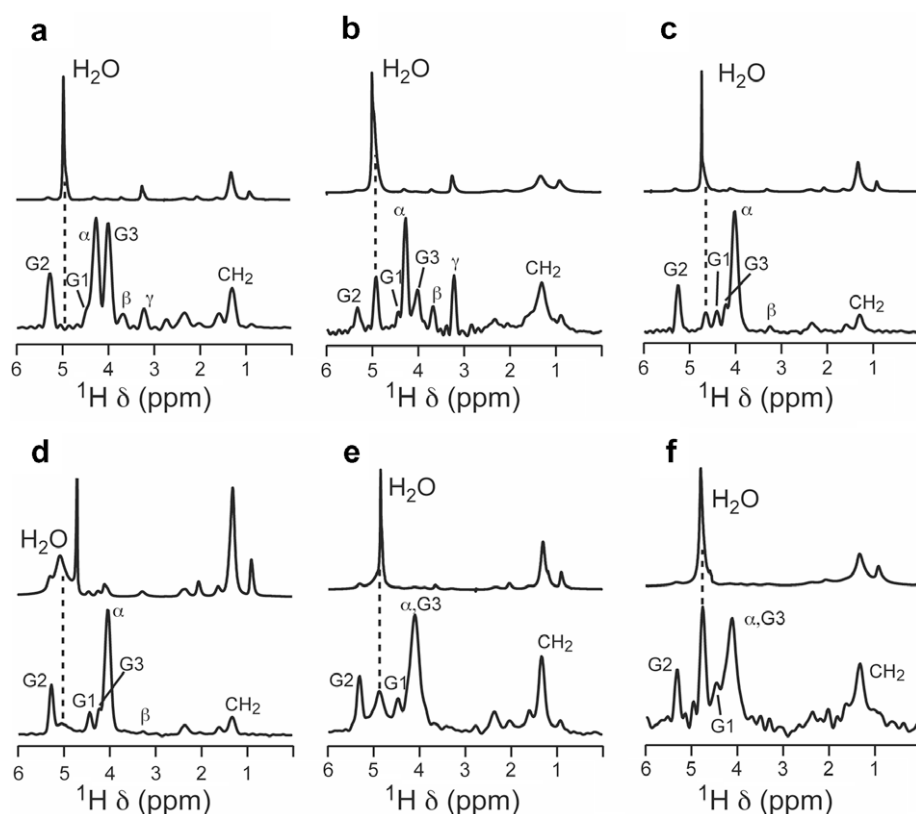


**Fig. 6.**  $^1\text{H}$  direct-excitation spectra (top) and cross sections from  $^1\text{H}$ - $^{31}\text{P}$  2D spectra (bottom) of various lipid membranes. Dashed lines guide the eye for the water peak. The most significant lipid peaks are assigned. (a) POPC membrane. (b) POPC/cholesterol membrane. (c) POPE membrane prepared from organic solution. (d) POPE membrane prepared from aqueous solution. (e) POPE/POPG membrane with TP-1. (f) POPE/POPG membrane with PG-1.

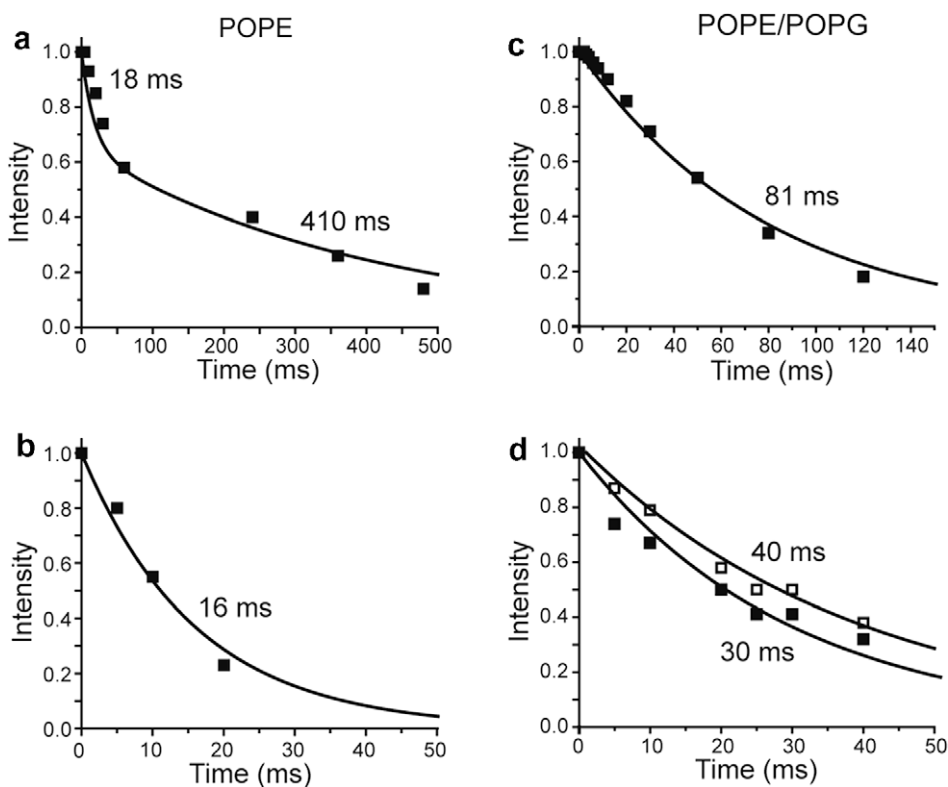


**Fig. 7.** Representative  $^1\text{H}$   $T_2$  curves from  $^1\text{H}$  1D and  $^1\text{H}$ - $^{31}\text{P}$  2D correlation spectra. Left column: POPE membrane. (a) 1D  $^1\text{H}$ -detected  $T_2$  decay of the narrow water peak, (b) 2D  $^{31}\text{P}$ -detected water  $^1\text{H}$   $T_2$  decay. Right column: POPE/POPG membrane. (c) 1D  $^1\text{H}$ -detected  $T_2$  decay of the water peak, (d) 2D  $^{31}\text{P}$ -detected water  $^1\text{H}$   $T_2$  decay. Filled squares: POPE. Open squares: POPG. Note that the time axis differs for the panels.

making a vesicle solution, subjecting it to several freeze-thaw cycles, then centrifuging the solution to give a pellet. This aqueous sample gave a broad water peak at 5.09 ppm (Fig. 6d), which is 0.43 ppm downfield from the broad water peak in the “organic” sample. This downfield water peak shows a  $T_2$  of 4.9 ms from the 2D experiments. The chemical shift of the lipid-associated water peak is the weighted average of the  $\text{NH}_3$  chemical shift and the water proton chemical shift. Lys  $\text{NH}_3$  protons in proteins protected from exchange have a chemical shift of 7–8 ppm [30], thus the downfield displacement of the inter-bilayer water peak in the aqueous POPE sample indicates that the amount of the inter-bilayer water is smaller in the aqueous sample than in the organic sample. Similarly, the shorter water  $T_2$  (4.9 ms) of the aqueous POPE sample compared to the organic sample (16 ms) can be attributed to the stronger influence of the  $\text{NH}_3$  proton dynamics in the exchange-average  $T_2$ . The  $^1\text{H}$   $T_2$ 's of the POPE headgroup decrease from  $\text{H}\alpha$  to  $\text{H}\beta$ , in contrast to the POPC headgroup, which has increasing  $T_2$ 's from  $\text{H}\alpha$  (27 ms) to  $\text{H}\beta$  (38 ms) and  $\text{H}\gamma$  (71 ms). The shorter  $^1\text{H}$   $T_2$  towards the end of the POPE headgroup most likely reflects intermolecular hydrogen bonding between  $\text{NH}_3^+$  and  $\text{PO}_4^-$  of neighboring lipid molecules, which restricts the headgroup mobility [31,32].

To obtain further insight into the nature of the POPE hydration-water, we examined the temperature dependence of the water cross peak in the 2D  $^1\text{H}$ - $^{31}\text{P}$  spectra. Fig. 8a shows the 1D cross sections of the organic POPE sample from 20 to 40 °C. The spectra were collected with identical scans and plotted on the same intensity scale after taking into account small CP efficiency differences. The water cross peak decreases with increasing temperature, with the most significant change occurring across the phase transition temperature of 25 °C. We also examined the mixing-time depen-

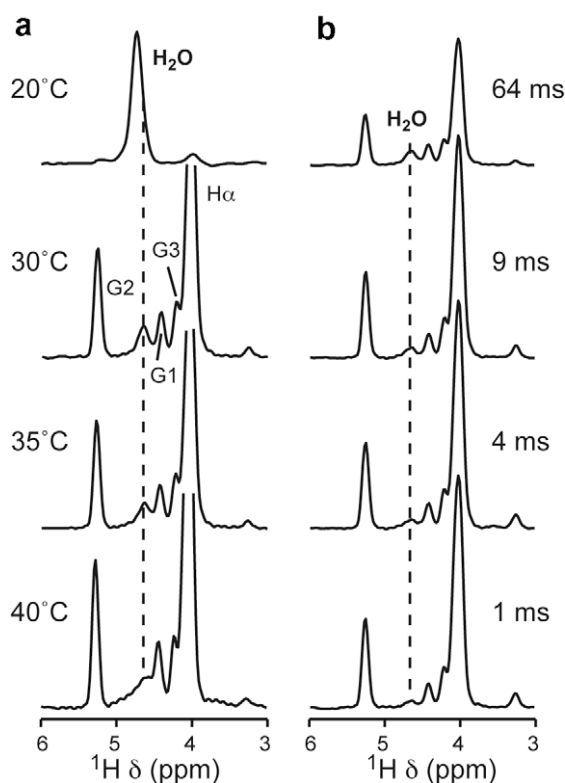


**Fig. 8.**  $^1\text{H}$  cross sections of the 2D  $^1\text{H}$ - $^{31}\text{P}$  spectra of hydrated POPE membrane. (a) Temperature dependence of the water cross peak intensity. Mixing-time was 64 ms for all spectra. (b) Mixing-time dependence of the water cross peak intensity at 30 °C.

dence of the water cross peak at 30 °C. The water cross peak was detected as early as 4 ms, as shown in Fig. 8b.

The POPG membrane shows a single water peak in the 1D spectra with a  $T_2$  of 32 ms and a water- $^{31}\text{P}$  cross peak in the 2D spectrum with a similar  $T_2$  of 30 ms. The high salt content of this lipid made the samples susceptible to rf heating and degradation so that variability in the cross peak intensity was observed. Buffering the membrane pH to 7 stabilized the sample to some extent and gave rise to a clear water- $^{31}\text{P}$  cross peak in the 64 ms 2D spectra. Mixing POPG with POPE lipids also created stable membranes, with reproducible water- $^{31}\text{P}$  cross peak intensities for both the POPE and POPG components. Fig. 5b shows the 2D spectrum of the POPE/POPG (3:2) membrane, exhibiting two well resolved  $^{31}\text{P}$  peaks along with their respective water cross peaks. The water  $^1\text{H}$   $T_2$  values are 30 ms for POPE and 40 ms for POPG (Table 1). Since the organic POPE membrane alone has a water  $T_2$  of 16 ms, the mixture result indicates that POPG lengthened the  $T_2$  of the POPE component.

### 3.3. Effect of cationic membrane peptides on inter-bilayer water $T_2$

We next examined the inter-bilayer water dynamics in the presence of two cationic membrane peptides. Tachyplesin-I (TP-I) and protegin-1 (PG-1) are Arg-rich cationic  $\beta$ -hairpin antimicrobial peptides that have recently been extensively characterized by solid-state NMR [19,20,33,34]. We measured the 2D  $^1\text{H}$ - $^{31}\text{P}$  spectra of POPE/POPG membrane containing these peptides. The  $^{31}\text{P}$  spectra no longer resolve the two lipids due to line broadening by the peptides. The  $^1\text{H}$  cross sections are shown in Fig. 6e, f. For the TP-I sample, the water cross peak is relatively broad and is lower than the main  $\text{H}\alpha/\text{G3}$  peak, similar to the other membranes. In contrast, the PG-1 sample exhibits a narrow and much stronger water peak with similar intensity as the  $\text{H}\alpha/\text{G3}$  peak. The  $T_2$  decay of these 2D-detected water peaks are shown in Fig. 9. Both peptide-containing samples exhibit much shorter water  $T_2$ 's than the pure POPE/POPG membrane: 3.3 ms for the TP-I sample and 0.4 ms (20%) and 12 ms (80%) for the PG-1 sample (Table 1).

The double-exponential nature of the water  $T_2$  decay for the PG-1-containing membrane is noteworthy. The large value of 12 ms is similar to the 1D-detected water  $T_2$  of 16 ms. Since the water cross peak is much higher in this sample than in the other samples, we assign the longer  $T_2$  component to highly mobile water between bilayers, whose magnetization is transferred to  $^{31}\text{P}$  as a result of the immobilized  $\beta$ -barrel assembly of PG-1 molecules [34]. In other words, the rigid peptide oligomers provide an efficient spin diffusion pathway from water to the lipid  $^{31}\text{P}$ . This assignment is confirmed by  $^{13}\text{C}$ - $^1\text{H}$  2D correlation spectra that correlate the  $^{13}\text{C}$

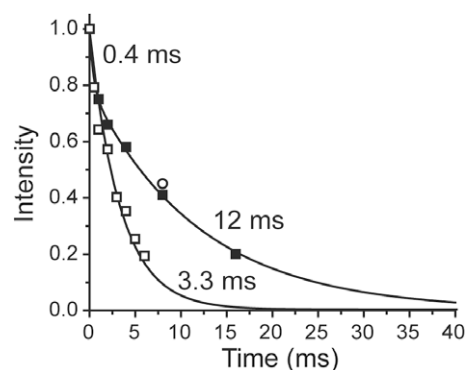


**Fig. 9.**  $^{31}\text{P}$ -detected water  $^1\text{H}$   $T_2$  decays of the POPE/POPG membrane containing cationic peptides. Open squares: TP-I. Filled squares: PG-1. Open circle: PG-1  $^{13}\text{C}$ -detected water cross peak intensity.

labeled residues in PG-1 with water  $^1\text{H}$ . The spectra showed similar water  $T_2$  dephasing as the  $^{31}\text{P}$ -detected experiment (Fig. 9), indicating that the same water molecules correlate with the lipid phosphate and with the peptide. The implication of this assignment is that the main water peak in the 1D  $^1\text{H}$  spectra of the PG-1 sample results from near-isotropic inter-bilayer water rather than bulk water outside the liposomes, similar to the POPC membrane. The absence of this long- $T_2$  in the TP-I sample can be attributed to the extensive dynamics of TP-I that prevents the detection of the highly mobile inter-bilayer water [19].

#### 4. Discussion

The lipid membranes used in this study are multilamellar vesicles that can have two very different types of water: bulk water outside the vesicles and inter-bilayer water within the vesicles. The observation of two partially resolved water  $^1\text{H}$  peaks in the slow-exchange limit with very different  $T_2$ 's supports the assignment of these two types of water.

The nature of water-membrane interaction has been extensively discussed in the literature. Early  $^2\text{H}$  NMR studies [4] led to the proposal of as many as three types of membrane-bound water, including tightly bound, weakly bound, and trapped water with fast exchange between them. More recent studies monitoring hydration-dependent  $^2\text{H}$  quadrupolar couplings indicate that the inter-bilayer water dynamics is a continuous function of hydration level [3]. A single quadrupolar splitting was observed for up to  $\sim 15$  water molecules per POPC molecule ( $n = 15$ ), above which a zero-frequency peak grows in that corresponds to bulk water in slow-exchange with the inter-bilayer water. The single-component nature of the  $^2\text{H}$  spectra below  $n = 15$  indicates that all inter-bilayer water undergoes rapid exchange on the  $^2\text{H}$  NMR timescale. Thus, phenomenologically, we do not further distinguish among inter-bilayer water molecules [3,35], even though the middle of the hydration layer has more isotropic water than the region near the membrane surface.

While water  $^2\text{H}$  NMR spectra of hydrated phospholipids give information on the residual quadrupolar coupling due to the inter-bilayer water anisotropy induced by the membrane, the 2D  $^1\text{H}$ - $^{31}\text{P}$  correlation technique is more sensitive to chemical exchange between water and labile lipid protons and to water-lipid dipolar interactions. The fact that the only lipid membrane that does not exhibit a water- $^{31}\text{P}$  correlation peak, POPC, is also the only lipid without any labile protons proves the essential role that chemical exchange plays in intermolecular magnetization transfer. POPE and POPG headgroups possess labile  $\text{NH}_3$  and OH protons, whose exchange rates have been measured in amino acids to be in the range of  $1000\text{--}4000\text{ s}^{-1}$  at  $36^\circ\text{C}$  and pH 7.0 [36]. The exchanged water  $^1\text{H}$  magnetization can then be relayed to  $\text{H}\alpha$  before cross-polarizing to  $^{31}\text{P}$ . This mechanism was termed chemically relayed nuclear Overhauser (or spin diffusion) effect, and its dependence on exchange rate and molecular motional correlation time have been analyzed in detail by 2D  $^1\text{H}$ - $^1\text{H}$  correlation NMR [37].

The rate of chemical exchange increases with temperature while the rate of dipolar magnetization transfer decreases with temperature. Thus, the change of the water cross peak intensity with temperature depends on the relative sensitivity of the two processes on temperature [36]. For the POPE membrane, we found that the water- $^{31}\text{P}$  cross peak increases as the temperature decreases and upon entering the gel-phase the cross peak intensity increases dramatically. This indicates that the more efficient  $^1\text{H}$  spin diffusion in the gel-phase membrane outweighs the reduction of the proton exchange rate at low temperature. However, this does not mean that exchange is unnecessary for the detection of the water- $^{31}\text{P}$  cross peak. At  $30^\circ\text{C}$ , the water- $\text{NH}_3$  exchange rate

of several thousand times per second [36] is much faster than the rate of  $^1\text{H}$  spin diffusion and cross-polarization from  $\text{NH}_3$  to  $^{31}\text{P}$ . The  $^1\text{H}$ - $^{31}\text{P}$  dipolar couplings to the nearest methylene groups of  $\text{H}\alpha$  and G3 are 200–300 Hz in liquid-crystalline PC and PE membranes [27], thus the magnetization transfer rate from the more remote  $\text{H}\gamma$  is at most several tens of hertz. Thus, the limiting factor in the chemically relayed nuclear Overhauser or spin diffusion process is the dipolar transfer rather than chemical exchange, and the temperature dependence of the dipolar transfer determines the overall intensity of the water cross peak. Recently it was shown that the 2D  $^1\text{H}$ - $^{31}\text{P}$  experiment is able to detect a water cross peak in sphingomyelin (SM) membranes but not in PC membranes [38]. While this difference is partly due to the rigidity of the SM membrane over the PC membrane, the presence of two labile protons in the SM backbone, which are absent in glycerophospholipid backbones, is almost certainly necessary for the observation of the water cross peak.

POPC differs from other membranes not only in having no labile protons in the headgroup, but also in having a single water signal with a  $T_2$  ( $\sim 60$  ms) that falls between the bulk water  $T_2$  ( $\sim 400$  ms) and inter-bilayer  $T_2$  (15–40 ms) of the other membranes. We assign this signal to inter-bilayer water for the following reasons. First, PC is much more hygroscopic than PE and PG lipids, as reflected by a thicker hydration layer and stronger repulsive hydration forces [2,31]. The higher hydration of PC compared to similarly zwitterionic PE lipids is attributed to the methylation of the primary amine in the PC headgroup, which weakens the attractive inter-bilayer forces resulting from hydrogen-bonded water bridges between apposing bilayers. Further, molecular dynamics simulations showed that the PC trimethylamine group has a much larger hydration shell than the PE amine [32,39] due to the absence of hydrogen bonding. Thus, more inter-bilayer water is required to hydrate PC than PE. Finally, our POPC sample has 15–18 water molecules per lipid based on  $^1\text{H}$  spectral integration. This is in the regime of little bulk water based on  $^2\text{H}$  NMR [3], thus supporting the assignment of the single water  $^1\text{H}$  peak to inter-bilayer water.

The lipid-correlated water  $^1\text{H}$   $T_2$ 's increase in the direction of POPC/cholesterol  $\leq$  POPE  $<$  POPG. Although it is tempting to interpret this trend as reflecting the interaction strengths between water and the various lipid membranes, the water  $T_2$  is the weighted average of the inter-bilayer water and labile lipid proton  $T_2$ 's, thus the lipid proton  $T_2$  affects the measured water cross peak  $T_2$ . For example, POPE  $\text{H}\beta$  has a shorter  $T_2$  ( $\sim 20$  ms in the organic sample and  $\sim 7$  ms in the aqueous sample) than the  $\text{H}\alpha$  protons ( $\sim 25$  ms in all samples), thus POPE  $\text{H}\gamma$  protons should have an even shorter intrinsic  $T_2$ , which should shorten the measured water cross peak  $T_2$ . Among all the lipid membranes studied here, the POPC/cholesterol bilayer is the most rigid and thus its water cross peak should have the largest contribution from direct dipolar effects between water and the lipid. Even so, the magnetization transfer pathway most likely involves an initial step of exchange from water to the cholesterol hydroxyl proton, followed by back transfer to the lipid chains and then to the lipid headgroup. Mixing-time dependence of the POPC/cholesterol 2D spectra (not shown) indicates that the water cross peak buildup is slower than the POPE membrane, consistent with a magnetization transfer pathway that involves lipid chain protons next to the rigid sterol rings.

Inclusion of cationic membrane peptides reduced the lipid-correlated water  $T_2$  to a few milliseconds. The number of labile protons in TP-I and PG-1 is similar. TP-I has 17 residues while PG-1 has 18, with the corresponding labile backbone amide protons. TP-I has five Arg residues and one Lys, each with exchangeable sidechain  $\text{NH}_n$  protons, while PG-1 contains six Arg residues. TP-I and PG-1 contain two and one hydroxyl-containing Tyr residues, respectively. However, the exposure of these labile protons to

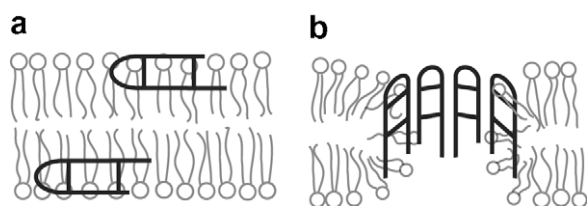


**Fig. 10.** Topological structures of TP-I and PG-1 in POPE/POPG membranes. (a) TP-I is monomeric and mobile and lies at the membrane-water interface. (b) PG-1 is transmembrane and forms immobilized  $\beta$ -barrels.

water and the efficiency of  $^1\text{H}$ - $^1\text{H}$  dipolar transfer differ significantly between the two peptides due to their different topological structures in the membrane. TP-I binds to the membrane-water interface near the glycerol backbone [33], is oriented roughly parallel to the membrane plane [40], and is highly dynamic [19]. In contrast, PG-1 forms immobilized transmembrane  $\beta$ -barrels in the anionic membrane [34,41] (Fig. 10), whose extensive intermolecular hydrogen bonding should shield some backbone NH protons from exchange. Thus, TP-I should experience more efficient water exchange than PG-1. But since the limiting factor in the water- $^{31}\text{P}$  cross peak detection is the dipolar transfer rate rather than the exchange rate, the immobilized PG-1 backbone transfers whatever amount of exchanged water magnetization to the lipid  $^{31}\text{P}$  much more efficiently than the dynamic TP-I. PG-1 thus shows a higher water cross peak than TP-I, and allows the observation of more isotropic inter-bilayer water, which is not observed in the TP-I sample.

## 5. Conclusion

The current 2D  $^1\text{H}$ - $^{31}\text{P}$  correlation study indicates that chemical exchange plays an essential role in the dynamics of hydration-water in lipid membranes. The presence of a  $^{31}\text{P}$ -correlated water peak in the 2D spectra requires exchangeable lipid protons, while the intensity of the cross peak is mainly determined by the  $^1\text{H}$ - $^1\text{H}$  dipolar transfer efficiency. The  $^{31}\text{P}$ -detected  $^1\text{H}$   $T_2$  of the inter-bilayer water is the exchange-averaged  $T_2$  of all inter-bilayer water and the labile lipid proton, and depends on the hydration level of the membrane and the property of the labile proton. Cholesterol facilitates the detection of the inter-bilayer water through its condensing effect on the membrane. Cationic membrane proteins affect the hydration-water dynamics through intermolecular hydrogen bonding and protein dynamics.

## Acknowledgments

The authors thank Prof. Alan J. Waring for providing the TP-I and PG-1 samples used in this study. T. Doherty is a grateful recipient of a Roy J. Carver Trust predoctoral training fellowship. The authors thank M. Tang for discussions and help with lipid  $^1\text{H}$  chemical shift assignment.

## References

- [1] V.A. Parsegian, N. Fuller, R.P. Rand, Measured work of deformation and repulsion of lecithin bilayers, *Proc. Natl. Acad. Sci. USA* 76 (1979) 2750–2754.
- [2] R.P. Rand, V.A. Arsegian, Hydration forces between phospholipid bilayers, *Biochim. Biophys. Acta* 988 (1989) 351–376.
- [3] F. Volke, S. Eisenblatter, J. Galle, G. Klose, Dynamic properties of water at phosphatidylcholine lipid-bilayer surfaces as seen by deuterium and pulsed field gradient proton NMR, *Chem. Phys. Lipids* 70 (1994) 121–131.
- [4] E.G. Finer, A. Darke, Phospholipid hydration studied by deuterium magnetic resonance spectroscopy, *Chem. Phys. Lipids* 12 (1974) 1–16.
- [5] A. Takahashi, T. Takizawa, Y. Nakata, A deuterium NMR study of the dynamics of water molecules bound tightly to the phosphate group in dipalmitoyl-phosphatidylcholine- $\text{D}_2\text{O}$  System, *J. Phys. Soc. Jpn.* 65 (1996) 635–642.
- [6] T.L. Ceckler, S.D. Wolff, V. Yip, S.A. Simon, R.S. Balaban, Dynamic and chemical factors affecting water proton relaxation by macromolecules, *J. Magn. Reson.* 98 (1992) 637–645.
- [7] K. Gawrisch, H.C. Gaede, M. Mihailescu, S.H. White, Hydration of POPC bilayers studied by  $^1\text{H}$ -PFM-MAS-NOESY and neutron diffraction, *Eur. Biophys. J.* 36 (2007) 281–291.
- [8] Z. Zhou, B.G. Sayer, D.W. Hughes, R.E. Stark, R.M. Epand, Studies of phospholipid hydration by high-resolution magic-angle spinning nuclear magnetic resonance, *Biophys. J.* 76 (1999) 387–399.
- [9] F. Volke, A. Pampel, Membrane hydration and structure on a subnanometer scale as seen by high resolution solid state nuclear magnetic resonance. POPC and POPC/C12EO4 model membranes, *Biophys. J.* 68 (1995) 1960–1965.
- [10] J. Fitter, R.E. Lechner, N.A. Dencher, Interactions of hydration water and biological membranes studied by neutron scattering, *J. Phys. Chem. B* 103 (1999) 8036–8050.
- [11] S. Konig, E. Sackmann, D. Richter, R. Zorn, C. Carlie, T.M. Bayerl, Molecular dynamics of water in oriented DPPC multilayers studied by quasielastic neutron scattering and deuterium-nuclear magnetic resonance relaxation, *J. Chem. Phys.* 100 (1994) 3307–3316.
- [12] R.H. Pearson, I. Pascher, The molecular structure of lecithin dihydrate, *Nature* 281 (1979) 499–501.
- [13] M.C. Wiener, S.H. White, Structure of a fluid DOPC bilayer determined by joint refinement of X-ray and neutron diffraction data III Complete structure, *Biophys. J.* 61 (1992) 434–447.
- [14] J.X. Cheng, S. Pautot, D.A. Weitz, X.S. Xie, Ordering of water molecules between phospholipid bilayers visualized by coherent anti-stokes raman scattering microscopy, *Proc. Natl. Acad. Sci. USA* 100 (2003) 9826–9830.
- [15] A.S. Ulrich, A. Watts, Molecular response of the lipid headgroup to bilayer hydration monitored by  $^2\text{H}$ -NMR, *Biophys. J.* 66 (1994) 1441–1449.
- [16] M. Hong, Oligomeric structure, dynamics, and orientation of membrane proteins from solid-state NMR, *Structure* 14 (2006) 1731–1740.
- [17] M. Hong, Structure, topology, and dynamics of membrane peptides and proteins from solid-state NMR spectroscopy, *J. Phys. Chem. B* 111 (2007) 10340–10351.
- [18] K. Gawrisch, N.V. Eldho, I.V. Polozov, Novel NMR tools to study structure and dynamics of biomembranes, *Chem. Phys. Lipids* 116 (2002) 135–151.
- [19] T. Doherty, A.J. Waring, M. Hong, Dynamic structure of disulfide-removed linear analogs of tachyplesin-I in the lipid bilayer from solid-state NMR, *Biochemistry* 47 (2008) 1105–1116.
- [20] S. Yamaguchi, A. Waring, T. Hong, R. Lehrer, M. Hong, Solid-state nmr investigations of peptide-lipid interaction and orientation of a beta-sheet antimicrobial peptide, protegrin, *Biochemistry* 41 (2002) 9852–9862.
- [21] K.L. Li, C.A. Tihal, M. Guo, R.E. Stark, Multinuclear and magic-angle spinning NMR investigations of molecular organization in phospholipid-triglyceride aqueous dispersions, *Biochemistry* 32 (1993) 9926–9935.
- [22] D. Huster, X.L. Yao, M. Hong, Membrane protein topology probed by  $^1\text{H}$  spin diffusion from lipids using solid-state NMR spectroscopy, *J. Am. Chem. Soc.* 124 (2002) 874–883.
- [23] J. Forbes, J. Bowers, X. Shan, L. Moran, E. Oldfield, M.A. Moscarello, Some new developments in solid-state nuclear magnetic resonance spectroscopic studies of lipids and biological membranes, including the effects of cholesterol in model and natural systems, *J. Chem. Soc. Faraday Trans. I* 84 (1988) 3821–3849.
- [24] J. Forbes, C. Husted, E. Oldfield, High-field, high-resolution proton “magic-angle” sample-spinning NMR spectroscopic studies of gel and liquid crystalline lipid bilayers and the effects of cholesterol, *J. Am. Chem. Soc.* 110 (1988) 1059–1065.
- [25] C. Husted, B. Montez, C. Le, M.A. Moscarello, E. Oldfield, Carbon-13 “magic-angle” sample-spinning nuclear magnetic resonance studies of human myelin, and model membrane systems, *Magn. Res. Med.* 29 (1993) 168–178.
- [26] M. Tang, A.J. Waring, R.I. Lehrer, M. Hong, Effects of guanidinium-phosphate hydrogen bonding on the membrane-bound structure and activity of an arginine-rich membrane peptide from solid-state NMR, *Angew. Chem. Int. Ed. Engl.* 47 (2008) 3202–3205.
- [27] M. Hong, K. Schmidt-Rohr, D. Nanz, Study of phospholipid structure by  $^1\text{H}$ ,  $^{13}\text{C}$ , and  $^{31}\text{P}$  dipolar couplings from 2D NMR, *Biophys. J.* 69 (1995) 1939–1950.
- [28] D. Huster, K. Arnold, K. Gawrisch, Investigation of lipid organization in biological membranes by two-dimensional nuclear Overhauser enhancement spectroscopy, *J. Phys. Chem.* 103 (1999) 243–251.
- [29] D. Huster, K. Gawrisch, NOESY NMR crosspeaks between lipid headgroups and hydrocarbon chains: spin diffusion or molecular disorder?, *J. Am. Chem. Soc.* 121 (1999) 1992–1993.
- [30] J. Iwahara, Y.S. Jung, G.M. Clore, Heteronuclear NMR spectroscopy for lysine  $\text{NH}(3)$  groups in proteins: unique effect of water exchange on  $(^{15}\text{N})$  transverse relaxation, *J. Am. Chem. Soc.* 129 (2007) 2971–2980.
- [31] R.P. Rand, N. Fuller, V.A. Parsegian, D.C. Rau, Variation in hydration forces between neutral phospholipid bilayers: evidence for hydration attraction, *Biochemistry* 27 (1988) 7711–7722.
- [32] F. Suits, M.C. Pitman, S.E. Feller, Molecular dynamics investigation of the structural properties of phosphatidylethanolamine lipid bilayers, *J. Chem. Phys.* 122 (2005) 244714.
- [33] T. Doherty, A.J. Waring, M. Hong, Membrane-bound conformation and topology of the antimicrobial peptide tachyplesin I by solid-state NMR, *Biochemistry* 45 (2006) 13323–13330.

- [34] R. Mani, S.D. Cady, M. Tang, A.J. Waring, R.I. Lehrer, M. Hong, Membrane-dependent oligomeric structure and pore formation of a  $\beta$ -hairpin antimicrobial peptide in lipid bilayers from solid-state NMR, *Proc. Natl. Acad. Sci. USA* 103 (2006) 16242–16247.
- [35] Z.J. Chen, L.C. Van Gorkom, R.M. Eppard, R.E. Stark, Nuclear magnetic resonance studies of lipid hydration in monomethyldioleoylphosphatidylethanolamine dispersions, *Biophys. J.* 70 (1996) 1412–1418.
- [36] E. Liepinsh, G. Otting, Proton exchange rates from amino acid side chains—implications for image contrast, *Magn. Reson. Med.* 35 (1996) 30–42.
- [37] F.J.M. van der Ven, H.G.J.M. Janssen, A. Graslund, C.W. Hilbers, Chemically relayed nuclear overhauser effects. Connectivities between resonances of nonexchangeable protons and water, *J. Magn. Reson.* 79 (1988) 221–235.
- [38] G.P. Holland, T.M. Alam, Unique backbone-water interaction detected in sphingomyelin bilayers with  $^1\text{H}/^{31}\text{P}$  and  $^1\text{H}/^{13}\text{C}$  HETCOR MAS NMR spectroscopy, *Biophys. J.* 95 (2008) 1189–1198.
- [39] C.F. Lopez, S.O. Nielsen, M.L. Klein, P.B. Moore, Hydrogen bonding structure and dynamics of water at the dimyristoylphosphatidylcholine lipid bilayer surface from a molecular dynamics simulation, *J. Phys. Chem.* 108 (2004) 6603–6610.
- [40] M. Hong, T. Doherty, Orientation determination of membrane-disruptive proteins using powder samples and rotational diffusion: a simple solid-state NMR approach, *Chem. Phys. Lett.* 432 (2006) 296–300.
- [41] J.J. Buffy, A.J. Waring, R.I. Lehrer, M. Hong, Immobilization and aggregation of antimicrobial peptide protegrin in lipid bilayers investigated by solid-state NMR, *Biochemistry* 42 (2003) 13725–13734.